

**Lecture 11-12: SIMPLIFIED ANALYSIS OF ARCJET OPERATION**

1. Introduction

These notes aim at providing order-of-magnitude results and at illuminating the mechanisms involved. Numerical precision will be sacrificed in the interest of physical clarity. We look first at the arc in a cooled constrictor, with no flow, expand the analysis to the case with flow, and then use the results to extract performance parameters for arcjets.

2. Basic Physical Assumptions

The gas conductivity model will be of the form

$$\sigma = \begin{cases} 0 & (T < T_e) & (T_e \approx 6000 - 7000K) \\ a(T - T_e) & (T > T_e) & (a \approx 0.8 \text{ Si/m/K}) \end{cases} \quad (1)$$

The thermal conductivity  $k$  of the gas will be modelled as a constant (with possibly a different value outside the arc). This is a fairly drastic simplification, since in  $H_2$  and  $N_2$   $k(T)$  exhibits very large peaks in the dissociation range (2000-5000K) and in the ionization range (12000-16000K). Because  $k$  always multiplies a temperature gradient, the combination  $d\Phi(T) = kdT$  is relevant, and so the proper choice of  $\bar{k}$  to be used is the averaged value

$$\bar{k} = \frac{1}{T_2 - T_1} \int_{T_1}^{T_2} kdT \quad (2)$$

over the range of temperatures intended.

The arc gas is modelled as ideal, even though its molecular mass shifts strongly and its enthalpy increases rapidly in the dissociation and ionization ranges. In particular,  $c_p = \left(\frac{\partial h}{\partial T}\right)_p$  has strong peaks, similar to those of  $k(T)$ , and, once again, we should use temperature-averaged values for it.

The arc is assumed quasi-cylindrical, with axial symmetry and with gradients which are much stronger in the radial than in the axial direction (similar to boundary layers). The flow region comprises three sub-domains:

- (a) The arc itself, for  $r < R_a(x)$ , corresponding to  $T > T_e$ . This is the only part carrying current.
- (b) The outer gas, not ionized and with  $T < T_e$ .

(c) For the case with coaxial flow, a thin transition layer between (a) and (b) may be necessary for accuracy, but will be ignored in our analysis.

### 3. Constricted Arc With No Flow

The typical arrangement is a strongly water-cooled cylindrical enclosure, made of mutually insulated copper segments, with the arc burning along its centerline (Fig. 1).

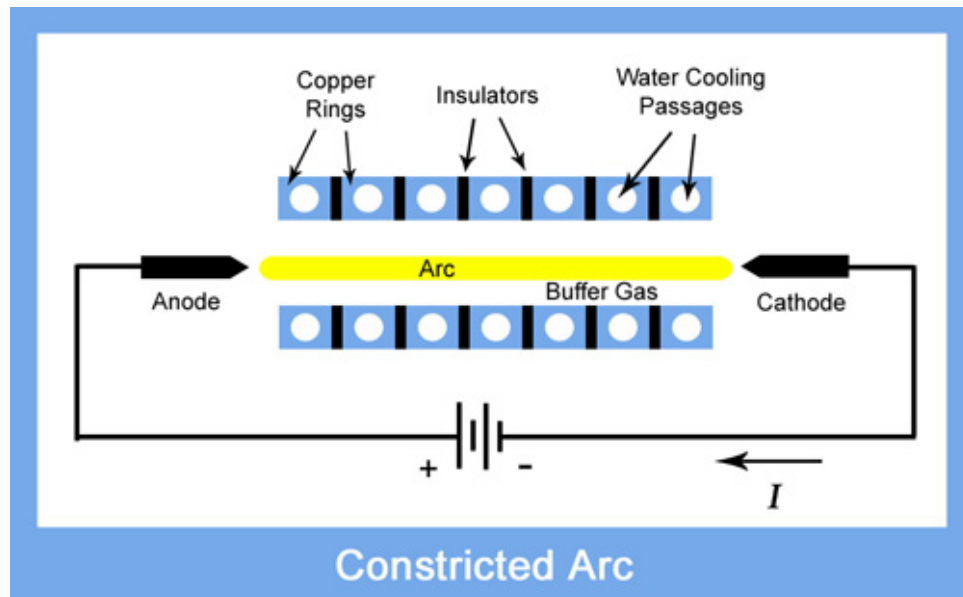


Fig. 1. Constricted Arc

Except for the near-electrode regions, the arc properties are constant along its length. In a cross-section, the axial electric field  $E = E_x$  is independent of radius as well, and  $E_r$  is small. The Ohmic dissipation rate is  $\vec{j} \cdot \vec{E}$  per unit volume, or  $\sigma E^2$ , since  $\vec{j} = \sigma \vec{E}$ . Here  $\sigma$  varies strongly inside the arc, from zero at  $r=R_a$  to a maximum  $\sigma_c$  at the centerline; as a rough approximation, we take  $\frac{1}{2} \sigma_c$  as a representative average, and so the amount of heat deposited ohmically per unit length is  $\frac{1}{2} \pi R_a^2 \sigma_c E^2$ . This heat must be conducted to

the arc's periphery, and so it must equal  $(2\pi R_a) \left( k \frac{\partial T}{\partial r} \right)_{r=R_a}$ . Representing the temperature

gradient  $R_a$  by (roughly)  $\left( -\frac{\partial T}{\partial r} \right)_{R_a} \cong 2 \frac{T_c - T_e}{R_a}$ , we obtain

$$\pi R_a^2 \frac{1}{2} \sigma_c E^2 = 2\pi R_a k_c 2 \frac{T_c - T_e}{R_a}$$

or 
$$E = 2 \sqrt{\frac{2k_c(T_c - T_e)}{\sigma_c}} \frac{1}{R_a} \quad (3)$$

and since  $\sigma_c = a(T_c - T_e)$ ,

$$\boxed{E = 2 \sqrt{2 \frac{k_c}{a}} \frac{1}{R_a}} \quad (4)$$

This important result indicates that the arc field, and hence its voltage, is inversely proportionally to its radius: the dissipation must increase if the arc is constrained more tightly, which improves its cooling. But note that  $R_a$  itself is not yet known, since it is only  $R$ , the constrictor diameter that is prescribed.

The total arc current is  $I = \int_0^R 2\pi r (\sigma E) dr$ . Once again, using  $\bar{\sigma} \cong \frac{1}{2} \sigma_c$ , we obtain

$$I = \pi R_a^2 \frac{\sigma_c}{2} E \quad (5)$$

and substituting (4) here,

$$I = \pi R_a^2 \frac{a(T_c - T_e)}{2} 2 \sqrt{2 \frac{k_c}{a}} \frac{1}{R_a}$$

$$\boxed{I = \pi \sqrt{2ak_c} (T_c - T_e) R_a} \quad (6)$$

Note also that, multiplying (4) and (6) together we obtain

$$EI = 4\pi k_c (T_c - T_e) \quad (7)$$

which is another way to express the heat balance. Its main message is that the arc centerline temperature  $T_c$  increases linearly with arc power per unit length,  $EI$ .

Everything covered so far will also apply later to the arc in a flow. The difference is in how the heat is evacuated from the arc periphery. With no flow, this must be accomplished by heat conduction through the buffer gas. If  $k_{out}$  denotes its thermal conductivity (probably much lower than  $k_c$ ), and if we ignore cylindrical effects, we must have equality of heat flux (per unit area) on both sides of the arc's edge:

$$k_c 2 \frac{T_c - T_e}{R_a} = k_{out} \frac{T_e - T_w}{R - R_a} \quad (8)$$

where  $T_w$  is the temperature of the constrictor's wall, controlled externally. Substituting  $T_c - T_e$  from (8) into (6),

$$I = \left( \pi R_a \sqrt{2ak_c} \right) \frac{1}{2} \frac{k_{out}}{k_c} \frac{R_a}{R - R_a} (T_e - T_w)$$

This is a quadratic equation for the arc radius  $R_a$ . To simplify algebra, introduce non-dimensional quantities:

$$I^* = \frac{I}{I_{ref}} \quad ; \quad I_{ref} = \pi R \sqrt{2ak_c} (T_e - T_w) \quad (9)$$

$$\lambda = \frac{k_{out}}{2k_c} \quad (10)$$

and 
$$r_a = \frac{R_a}{R} \quad (11)$$

and so 
$$I^* = \lambda \frac{r_a^2}{1 - r_a} \quad (11)$$

Solving for  $r_a$ ,

$$r_a = \frac{2}{1 + \sqrt{1 + \frac{4\lambda}{I^*}}} \quad (12)$$

which approaches 1 from below as  $I^*$  becomes large. We can now obtain other quantities of interest. From (8),

$$\frac{T_c - T_e}{T_e - T_w} = \frac{1}{2} \frac{k_{out}}{k_c} \frac{R_a}{R - R_a} = \lambda \frac{r_a}{1 - r_a} = \frac{2\lambda}{\sqrt{1 + \frac{4\lambda}{I^*}} - 1}$$

or, rearranging,

$$\boxed{\frac{T_c - T_e}{T_e - T_w} = \frac{1 + \sqrt{1 + \frac{4\lambda}{I^*}}}{2} I^*} \quad (13)$$

which shows how  $T_c$  eventually increases linearly with  $I^*$ , but its variation is faster ( $\approx \sqrt{I^*}$ ) at low current.

The field itself follows from (4). Define a non-dimensional field

$$E^* = \frac{E}{E_{ref}} \quad ; \quad E_{ref} = 2\sqrt{\frac{2k_c}{a}} \frac{1}{R} \quad (14)$$

and then

$$\boxed{E^* = \frac{1}{r_a} = \frac{1 + \sqrt{1 + \frac{4\lambda}{I^*}}}{2}} \quad (15)$$

which indicates a decreasing field (and voltage) as the current increases.

These results are summarized in Fig. 2, calculated with  $\lambda = 1/4$ .

The negative slope of the line  $E^* = f(I^*)$  is typical of arc discharges, and creates some difficulties in their operation. We note first that the increase of  $E^*$  as  $I^*$  decreases does not continue indefinitely; below some current level, the thermal power input to the electrodes (particularly the cathode) is insufficient to sustain the electron emission required, and the discharge transitions to a different mode, probably an “anomalous glow discharge”.

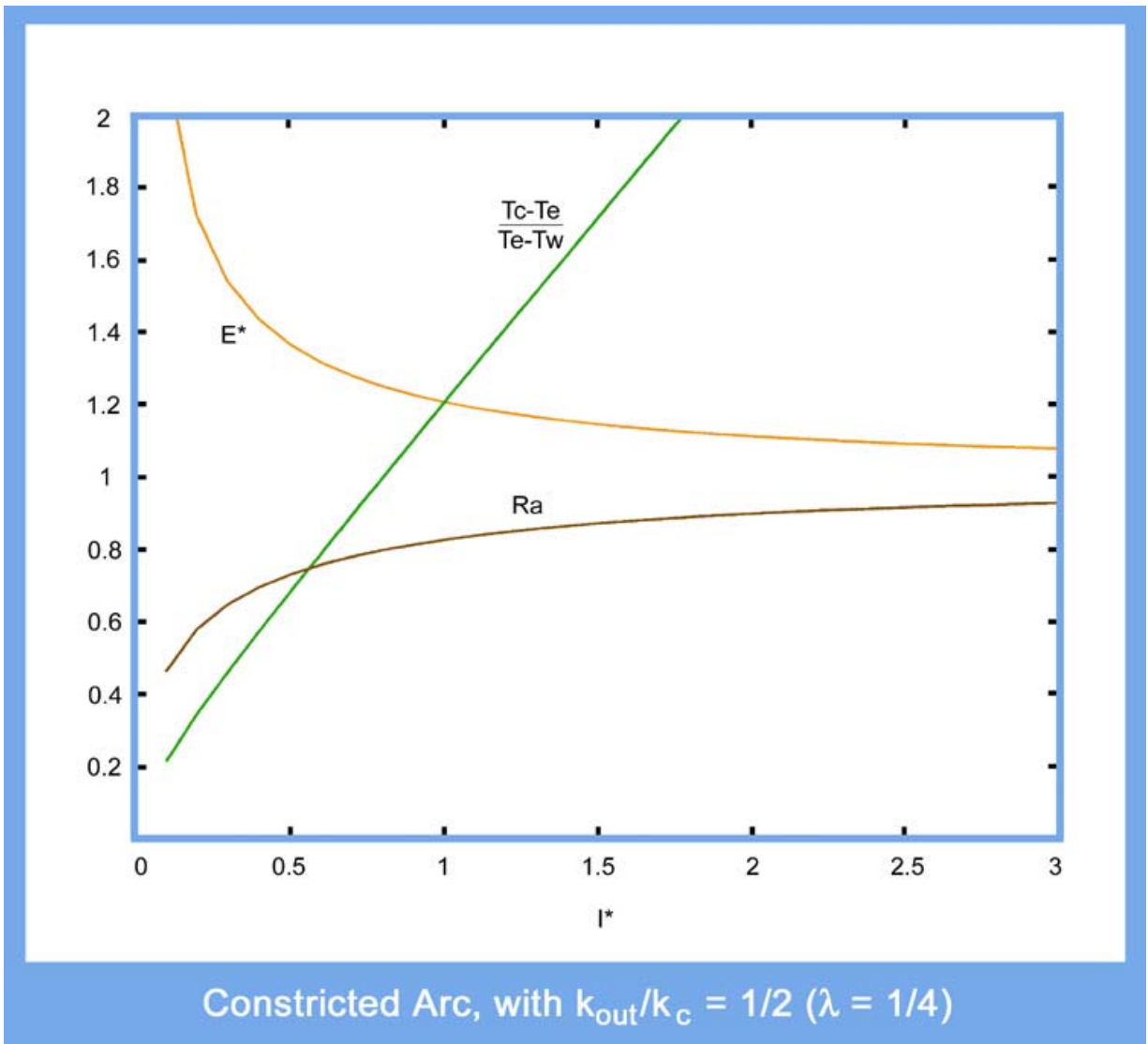


Figure 2

This happens at current levels in the micro- to milliampere, and the complete V-I curve of an arc then appears as in Fig. 3:

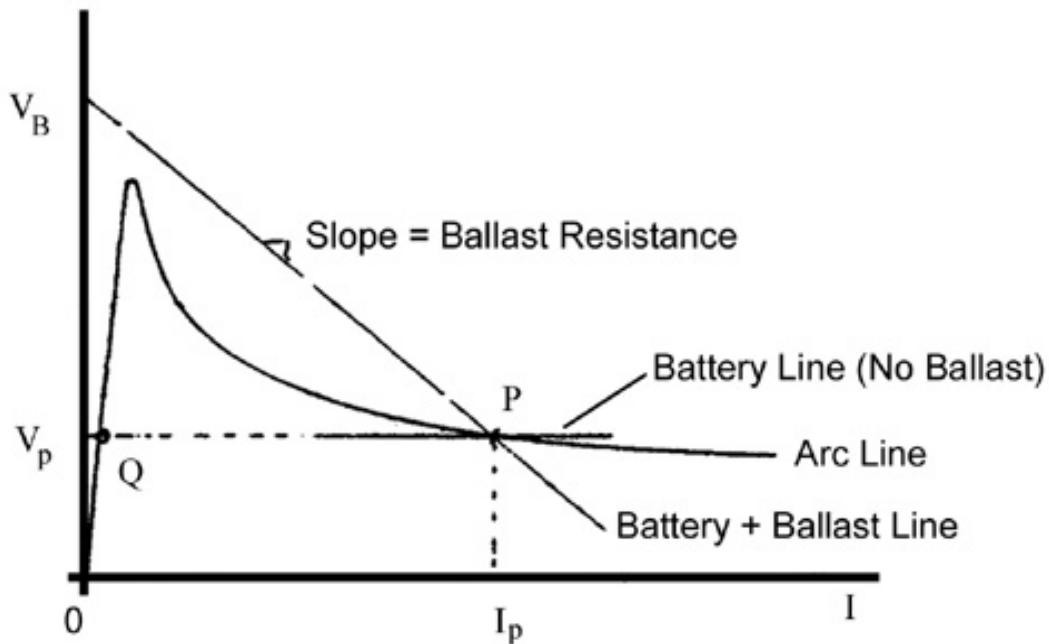


Figure 3. Complete V-I Arc Characteristic

Assuming we wish to operate at point P on this line, if we simply connect the arc to a constant-voltage source, such as a battery, we obtain an unstable arrangement. This is because, if current, say, increases slightly above  $I_p$ , the arc would now demand less than the equilibrium voltage  $V_p$  which the source delivers, and so  $I$  would increase even further, and run away (to the supply limit, or to destruction). Conversely, any negative current fluctuation would cause a rapid snap back to the stable operating point Q (at very low current).

One solution is to insert a series resistance  $R_B$  (“ballast”) and increase the source open-circuit voltage to, say  $V_B$  (Fig. 3). Since the voltage available to the arc is now  $V_B - R_B I$ , the supply line cuts the arc line from above (Fig. 3), and repeating the argument we notice stable operation at P. But, of course, we dissipate in the ballast the power

$I_p (V_B - V_p)$ , which leads to inefficient operation. Notice, however, that AC arcs can be efficiently ballasted by a series inductor, the familiar “choke” in fluorescent fixtures.

Alternatively, one can use a current-regulated power supply, provided its regulating speed and authority are high enough. For space applications, this takes the form of high frequency solid state switching regulators, capable of stabilizing the arc with minimal losses (efficiency > 90%). A series inductor can help with the high frequency part of the fluctuation spectrum.

#### 4. Constricted Arc in a Parallel Flow

This is the desired configuration for an arcjet (Fig. 4). Here, the heat which arrives through internal conduction at the arc periphery is removed by convection in the outer flow. The gas which comes into contact with the arc is heated as it moves axially, and some of it reaches the ionization threshold  $T_e$  and becomes part of the arc itself. This means the arc grows with distance, just as the thermal boundary layer adjacent to a heated surface does.

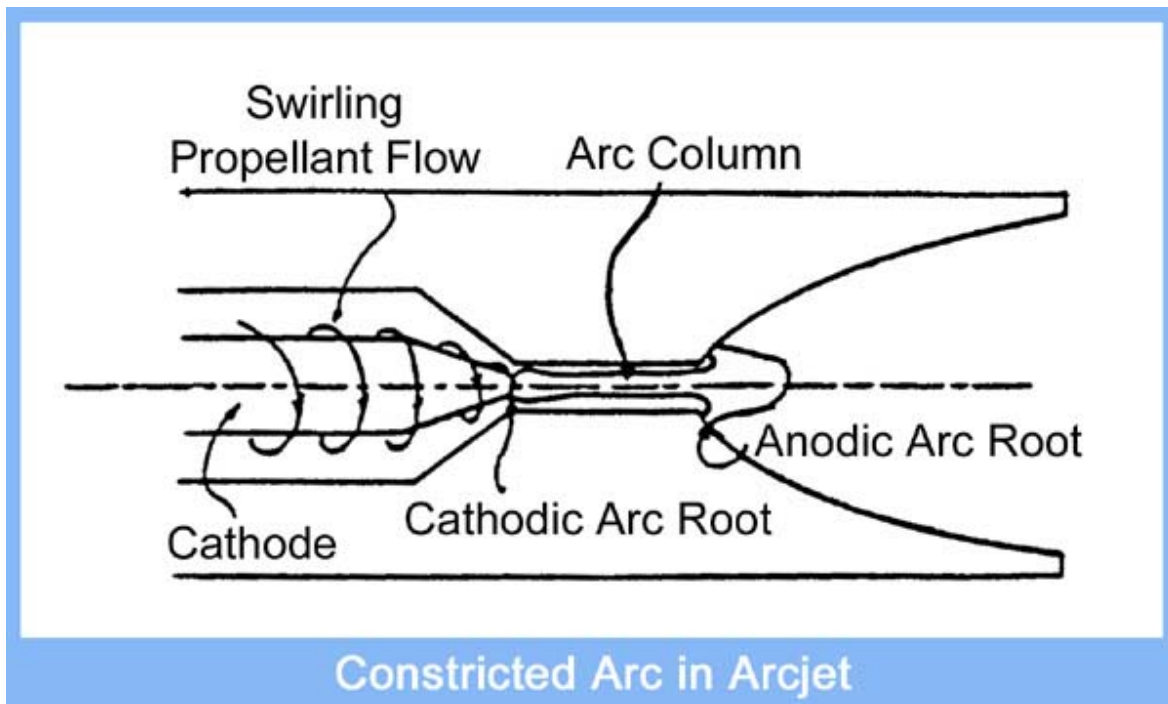


Fig. 4. Constricted Arc in Arcjet

Let  $(\rho u)_e$  be the axial mass flux at the arc's edge ( $r=R_a$ ). The amount of "new" arc flow in a distance  $dx$  is then  $(\rho u)_e 2\pi R_a \frac{dR_a}{dx} dx$ . The energy absorbed in heating this gas from  $T_{out}$  (the buffer gas temperature) to  $T_e$  must be supplied by the arc power dissipation. Using (7), we then have

$$(\rho u)_e 2\pi R_a \frac{dR_a}{dx} c_p (T_e - T_{out}) = 4\pi k_c (T_c - T_e) \quad (16)$$

In order to estimate  $(\rho u)_e$ , we now make the further assumption that the quantity  $\rho u^2$  is independent of r at a given  $x$ . This is motivated by the observation that in a parallel,

inviscid flow,  $p + \rho u^2$  remains constant along the streamlines, while  $p$  is itself independent of  $r$ . Thus  $\rho u^2$  develops gradually at the expense of  $p$ , and this should lead to a radius-independent  $\rho u^2$ . Our flow is not exactly parallel or inviscid, but the approximation (verified from numerical 2-D solutions) is good enough for the present purposes.

We then have,

$$\rho u = \sqrt{p(\rho u^2)} = \frac{\sqrt{p(\rho u^2)}}{\sqrt{R_g T}} \quad (17)$$

showing that most of the mass flow must occur in the cool, outside gas, since the numerator in (17) is independent of  $r$ .

We then have,

$$\frac{(\rho u)_e}{(\rho u)_{out}} = \sqrt{\frac{T_{out}}{T_e}} \quad (18)$$

and the problem is now to calculate the gas flux  $(\rho u)_{out}$  in the buffer gas. The simplest possible approximation is to state that all of the gas flow is carried by this uniform buffer flow:

$$(\rho u)_{out} \cong \frac{\dot{m} \dot{X}}{\pi(R^2 - R_a^2)} \quad (19)$$

This yields

$$(\rho u)_e \cong \frac{\dot{m} \dot{X}}{\pi(R^2 - R_a^2)} \sqrt{\frac{T_{out}}{T_e}} \quad (20)$$

and, substituting into (16),

$$\frac{\dot{m} \dot{X}}{\pi(R^2 - R_a^2)} \sqrt{\frac{T_{out}}{T_e}} R_a \frac{dR_a}{dx} c_p (T_e - T_{out}) \cong 2k_c (T_c - T_e)$$

The quantity  $T_c - T_e$  depends on current and arc radius through Eq. (6).

Substituting,

$$\frac{\dot{m}\dot{X}}{\pi(R^2 - R_a^2)} \sqrt{\frac{T_{out}}{T_e}} R_a \frac{dR_a}{dx} c_p (T_e - T_{out}) \cong 2k_c \frac{I}{\pi \sqrt{2ak_c} R_a}$$

or

$$\frac{R_a^2}{R^2 - R_a^2} \frac{dR_a}{dx} = \frac{I \sqrt{\frac{2k_c}{a}} \sqrt{\frac{T_e}{T_{out}}}}{\dot{m}\dot{X}_p (T_e - T_{out})} \quad (21)$$

We again non-dimensionalize using  $I^*$ ,  $r_a$  as in (9), (11), plus a non-dimensional distance

$$x^* = \frac{x}{x_{ref}} \quad ; \quad x_{ref} = \frac{1}{2\pi} \frac{\dot{m}\dot{X}_p}{k_c} \sqrt{\frac{T_{out}}{T_e}} \quad (22)$$

with the result

$$\frac{r_a^2}{1 - r_a^2} \frac{dr_a}{dx^*} = \left( \frac{T_e - T_w}{T_e - T_{out}} \sqrt{\frac{T_w}{T_{out}}} \right) I^* \quad (23)$$

Since  $T_e$  is much greater than either  $T_w$  or  $T_{out}$  (which are similar) the temperature function on the right of (23) is close to 1, and will be ignored. Integrating (23), from  $r_a(o) = r_{ao}$  gives

$$x^* = \frac{1}{I^*} \left[ \ln \sqrt{\frac{1+r_a}{1-r_a}} - r_a \right]_{r_{ao}}^a \quad (24)$$

which is an inverse expression for radius vs. distance.

For  $r_a \ll 1$  the bracketed quantity in (24) is approximated by Taylor expansion as  $\frac{r_a^3}{3}$  which indicates rapid arc growth near its upstream (cathodic) end. Therefore it is allowable to use  $r_{ao} \cong 0$  in (24), with only minor effect on length.

The remaining important question is the determination of the pressure (either P, the total pressure from upstream, or the pressure  $P_{ce}$  at the constrictor exit) required for a flow  $\dot{m}\dot{X}$ , given the current I and geometrical data. For this, recall the assumption that the outside layer carries all the flow, and is undisturbed, because the arc heat has not yet penetrated to it. It then is a subsonic ideal gas flow in a contracting area  $\pi(R^2 - R_a^2)$ , and will reach sonic conditions at the constrictor exit, provided the initial nozzle divergence

is sufficient. In terms of the total pressure  $P_t$ , and temperature  $T_t$  (the upstream conditions), we must then have

$$\dot{m}^* = \Gamma \frac{P_t \pi (R^2 - R_{a,L})}{\sqrt{R_g T_t}} \quad (25)$$

$$\text{with } \Gamma = \sqrt{\gamma} \left( \frac{2}{\gamma + 1} \right)^{\frac{\gamma+1}{2(\lambda-1)}} \cong \frac{2}{3} \quad (26)$$

and with  $R_{a,L}$  representing the arc radius at x-L, the constrictor exit. A non-dimensional mass flow rate is defined as

$$\dot{m}^* = \frac{\dot{m}}{\dot{m}_{ref}} \quad ; \quad \dot{m}_{ref} = \Gamma \frac{P_t \pi R^2}{\sqrt{R_g T_t}} \quad (27)$$

and (25) reads then

$$\dot{m}^* = 1 - r_{a,L}^2 \quad (28)$$

These equations can be used in a variety of ways. Two of them are:

- (a) “Design” mode. Given  $P_t$ ,  $T_t$ ,  $I$ ,  $\dot{m}^*$ ,  $R$ , etc., find the required constrictor length  $L$  (or given  $L$ , find  $R$ ).
- (b) “Analysis” mode. Given  $T_t$ ,  $I$ ,  $\dot{m}^*$ ,  $L$ ,  $R$ , etc., find the pressure  $P_t$ . This then will determine the thrust.

### Example

For  $H_2$  gas, say  $a=0.8\text{Si/m/K}$ ,  $T_e=7000\text{K}$  and (eyeballing from the chart handed out in class),  $k \cong 7w/m/K$ . Use also  $c_p \cong 5 \times 10^4 J/Kg$ . If the constrictor dimensions are  $R=1.25\text{mm}$ ,  $L=8\text{mm}$ , and the buffer gas temperature is  $T_t \cong T_w \cong 500\text{K}$ , find the chamber pressure  $P_t$  at operating conditions  $\dot{m}^* = 0.1g/s$ ,  $I = 100\text{A}$ .

From (9),

$$I_{ref} = \pi \times 1.25 \times 10^{-3} \sqrt{2 \times 0.8 \times 7(7000 - 500)} = 85.4 \text{Amp}$$

$$I^* = \frac{100}{85.4} = 1.171$$

From (22)

$$x_{ref} = \frac{1}{2\pi} \frac{10^{-4} \times 5 \times 10^4}{7} \sqrt{\frac{500}{7000}} = 0.0304m$$

$$x^* = \frac{8}{30.4} = 0.263$$

From (24) then,

$$0.263 = \frac{1}{1.171} \left( \ell n \sqrt{\frac{1+r_{a,L}}{1-r_{a,L}}} - r_{a,L} \right)$$

which can be solved to  $r_{a,L}=0.805$ . Then, from (28)

$$\dot{m}^* = 1 - (0.805)^2 = 0.352 \quad ; \quad \dot{m}_{ref} = \frac{\dot{m}}{\dot{m}^*} = 0.284g/s$$

and from (25), (27),  $\Gamma(\gamma = 1.4) = 0.685$ , and

$$\dot{m}_{ref} = 0.685 \frac{P_t \pi (1.25 \times 10^{-3})^2}{\sqrt{\frac{8.31}{0.002} \times 500}} = 2.33 \times 10^{-9} P_t$$

$$\left[ P_t = \frac{0.284 \times 10^{-3}}{2.33 \times 10^{-9}} = 1.218 \times 10^5 N/m^2 = 1.202 atm \right]$$

From the paper AIAA-90-2531, the experimental value under these conditions is 1.16 atm, a good agreement. Repeating for other conditions would yield:

$\dot{m}(g/s)$	I(A)	$\frac{R_a}{R}$ (calc.)	$P_t(atm)$ (calc.)	$P_t(atm)$ (data)
0.1	100	0.805	1.20	(1.16)
0.2	100	0.686	1.60	(1.80)
0.3	100	0.616	2.05	(2.55)
0.1	60	0.718	0.88	(0.97)
0.1	150	0.870	1.74	(1.28)

Table 1

As expected, the agreement is only approximate, but trends are well predicted. Notice how increasing the flow reduces the arc radius (higher buffer layer density, less radius growth for similar heated mass). The increase in pressure with current is also indicated, but the model exaggerates the effect.

## 5. VOLTAGE AND POWER CALCULATION

The axial field is still related to arc radius by  $E^* = \frac{1}{r_a}$ . The voltage accumulated in the constrictor is then

$$V_{const.} = \int_0^L E dx = E_{ref} x_{ref} \int_0^L E^* dx^*$$

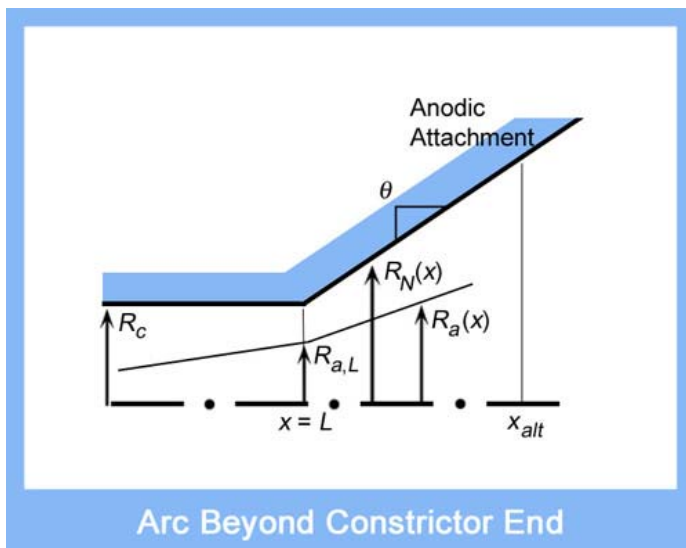
changing integration variable to  $r_a$ ,  $dx^* = dr_a / \left( \frac{dr_a}{dx^*} \right)$ ,

$$V_{const.}^* \equiv \frac{V_{const.}}{E_{ref} x_{ref}} = \int_0^{r_{a,L}} \frac{1}{r_a} \frac{r_a^2}{I^* (1 - r_a^2)} dr_a$$

which integrates to

$$V_{const.}^* = \frac{1}{2I^*} \ln \left( \frac{1}{1 - r_{a,L}^2} \right) \quad (29)$$

One difficulty in modeling arcjets is the question of precisely where the arc attaches to the nozzle. This is still largely an unresolved issue, but it is experimentally observed often that the attachment point is well downstream of the constrictor exit, in the supersonic part of the flow. We will construct a crude model only for the voltage drop in this portion.



The assumption will be that the arc growth beyond the constrictor end is simply due to the general flow expansion:

$$R_a(x > L) \cong R_{a,L} \frac{R_N(x)}{R_c} \quad (30)$$

In addition, the axial field is still governed by Eq. (4).

Figure 5

Then

$$\Delta V_{nozzle} = 2\sqrt{2\frac{k_c}{a}} \int_L^{x>L} \frac{dx}{R_a(x)}$$

and since  $dx = \frac{dR_N}{\tan \mathcal{G}}$ , using (3) we can integrate

$$\Delta V_{nozzle} \cong 2\sqrt{2\frac{k_c}{a}} \frac{1}{r_{a,L} \tan \mathcal{G}} \ln\left(\frac{R_{N,att.}}{R_c}\right)$$

which can be evaluated if an empirical value for  $R_{N,att.}$  (or for  $x_{att.}$ ) is available.

In addition, the near-anode region of the arc, where electrons must traverse the normally cool wall boundary layer, is very resistive (although Ohmic heating does elevate the electron temperature there). As a consequence, an additional anodic drop occurs, which, once again, is beyond this model's capabilities. Approximate empirical values are

$$\Delta V_{anode} \cong \begin{cases} 25 \text{ V water - cooled copper anode} \\ 0 - 10 \text{ V Hot anode} \end{cases} \quad (33)$$

Finally, a similar, but smaller cathodic drop also occurs near the cathode tip, this time due to the necessity for the electrons emitted from the cathode to gather sufficient energy to start the ionization process. This cathode drop is of the order of 1/2 to 1 times the gas ionization potential:

$$\Delta V_{cathode} \cong 6 - 12 \text{ V} \quad (34)$$

Example. We continue with the conditions of the Example in Sec. 4:  $H_2$ ,  $R_c=1.25\text{mm}$ ,  $L=8\text{mm}$ ,  $I=100\text{A}$ ,  $\dot{m} = 0.1\text{g/s}$ ,  $T_w=500\text{K}$ . We had found  $T_{a,L} = 0.805$ ,  $I^* = 1.171$  for these conditions. Suppose now we have a  $\mathcal{G} = 20^\circ$  nozzle, and that attachment is observed 4mm downstream of the constrictor:

$$\frac{R_{att.}}{R_c} = 1 + \frac{4 \tan 20^\circ}{1.25} = 2.17$$

We also have  $E_{ref} = 2\sqrt{\frac{k_c}{a}} \frac{1}{R_c} = 6690\text{Volt}$ , and  $x_{ref} = 0.0304\text{m}$ . Using now Eqs. (29)-(34), we estimate

$$V_{const.} = \frac{6690 \times 0.0304}{2 \times 1.171} \ln \frac{1}{1 - (0.805)^2} = 90.7\text{Volt}$$

$$V_{nozzle} = 2\sqrt{\frac{2 \times 7}{0.8}} \frac{1}{0.805 \tan 20^\circ} \ln(2.17) = 31.5 \text{ Volt}$$

$$\Delta V_{anode} \cong 25 \text{ Volt}$$

$$\Delta V_{cathode} \cong 8 \text{ Volt}$$

$$\text{Total: } V = 154.7 \text{ Volt}$$

The experimental value (AIAA 90-2531) is 148 Volt.

Again, we can repeat this process for a few other conditions, as we did in Table 1, with the results:

Table 2

$\dot{m}(\text{g/s})$	I(A)	$V_{CONSTR.}(V)$	$V_{NOZZ.}(V)$	$\Delta V_{a+c}(V)$	V(V)	$V_{\text{exper.}}(V)$
0.1	100	90.7	31.5	33	154.7	(148)
0.2	100	110.5	37.0	33	180.5	(180)
0.3	100	124.3	41.2	33	198.5	(203)
0.1	60	104.8	35.3	33	173	(160)
0.1	150	81.9	29.1	33	144	(142)

The power absorbed by the thruster is simply now the product of the given current and the total calculated voltage

$$P = VI \tag{35}$$

## 6. THRUST CALCULATION

Following the arc attachment, near the constrictor exit, the gas is very non-uniform in temperature, having “inherited” the arc’s thermal distribution. From that point, each streamline will ideally expand in the nozzle to the nozzle exit pressure,  $P_e$ . Since the starting point of the expansion had a uniform pressure and a uniform Mach number (despite the non-uniform T), and the exit condition also has uniform pressure, we must also have a uniform exit Mach number,  $M_e$ . Each streamtube expands in accordance to the same Mach number all across, and so the overall area ratio (exit/constrictor exit) is, as usual

$$\frac{A_e}{A_{ce}} = \frac{1}{M_e} \left( \frac{1 + \frac{\gamma-1}{2} M_e^2}{\frac{\gamma+1}{2}} \right)^{\frac{\gamma+1}{2(\gamma-1)}} \quad (36)$$

and the exit pressure is related to the stagnation pressure as

$$\frac{P_e}{P_t} = \frac{1}{\left( 1 + \frac{\gamma-1}{2} M_e^2 \right)^{\gamma/\gamma-1}} \quad (37)$$

We can then easily calculate the thrust by considering the exit plane:

$$F = (\rho_e u_e^2 + P_e) A_e = P_e A_e (1 + \gamma M_e^2) \quad (38)$$

The usually defined thrust coefficient is then

$$c_F = \frac{F}{P_t A_{ce}} = \frac{P_e}{P_t} \frac{A_e}{A_{ce}} (1 + \gamma M_e^2) \quad (39)$$

and, as can be verified from (36) and (37), this is identical to what would be obtained for an ordinary rocket for the same  $M_e$  or area ratio.

It is interesting, however, to examine the specific impulse  $c$  as well, or the “characteristic velocity”,  $c^* = c/c_F$ . The mass flow rate can be calculated at the (sonic) constrictor exit:

$$\dot{m} \dot{X} = \left( \int \rho u dA \right)_{ce} = P_{ce} \sqrt{\frac{\gamma}{R_g}} \int \frac{dA_{ce}}{\sqrt{T_{ce}}} \quad (40)$$

or, in terms of averaged quantities  $\left\langle \psi \right\rangle = \frac{1}{A} \int \psi dA$

$$\dot{m} \dot{X} = P_{ce} A_{ce} \sqrt{\frac{\gamma}{R_g}} \left\langle \frac{1}{\sqrt{T_{ce}}} \right\rangle \quad (41)$$

For a given  $P_t$  and  $A_{ce}$ ,  $F=c_F P_t A_{ce}$  is as it would be if the temperature were uniform in the constrictor. But (41) indicates that  $\dot{m} \dot{X}$  is affected by the  $T_{ce}$  non-uniformity, and so will then  $c = F/\dot{m} \dot{X}$ . For comparison, consider a uniformly heated gas stream that would use the same power per unit mass, and hence would have the same average temperature  $\left\langle T_{ce} \right\rangle$ .

This hypothetical rocket would have a specific impulse  $c_{\langle \rangle}$ , and

$$\frac{c}{c_{\langle \rangle}} = \frac{\dot{m}_{\langle \rangle}}{\dot{m}} = \frac{\left(1/\sqrt{\langle T_{ce} \rangle}\right)}{\left\langle \frac{1}{\sqrt{T_{ce}}} \right\rangle} = \frac{1}{\left(\sqrt{\langle T_{ce} \rangle}\right) \left\langle \frac{1}{\sqrt{T_e}} \right\rangle} \quad (42)$$

It can be proven in general that the quantity in the denominator of (42) is always greater than unity, unless  $T_{ce}$  is uniform, and so our arcjet will deliver lower specific impulse than if the heating were uniform. This is a manifestation of a very general principle in propulsion: the highest thrust per unit power (or the least power per unit thrust) is achieved when the exit stream is uniform.

As an example, suppose the inner 1/2 of the constrictor exit area is at 10,000K the rest at 1000K. We then have  $\langle T \rangle = \frac{10,000 + 1000}{2} = 5,500K$ ,

$$\left\langle \frac{1}{\sqrt{T}} \right\rangle = \frac{\frac{1}{\sqrt{10,000}} + \frac{1}{\sqrt{1000}}}{2} = 0.02081. \text{ This gives}$$

$$\frac{c}{c_{\langle \rangle}} = \frac{1}{74.16 \times 0.02081} = 0.648$$

which is a substantial thrust loss.

Performance example. We return to the hydrogen arcjet at the 0.1g/s, 100 Amp condition. The area ratio is now given as  $\frac{A_e}{A_{ce}} = 100$ . We use  $\gamma = 1.35$  to represent the partially heated gas, and from (36),  $M_e = 6.338$ . From this, and the previously calculated  $P_i = 1.20\text{atm}$  (Table 1), we find  $P_e = 0.000324\text{atm}$ . The thrust, from (38) is then

$$F = 0.890\text{N}$$

The experimental value (AIAA 90-2531) at the power  $P = 100A \times 154.8V = 15.5KW$  is  $F = 0.751\text{N}$ . Our overprediction is probably related to ignoring friction losses and boundary layer blockage, not entirely negligible at the small Reynolds numbers of these devices.

Once the power and the thrust are calculated, the efficiency follows from

$$\eta = \frac{1}{2} \frac{F^2}{\dot{m}P} = \frac{1}{2} \frac{0.890^2}{(10^{-4})(1.55 \times 10^4)} = 0.256$$

and the specific impulse is

$$I_{sp} = \frac{1}{9.81} \frac{0.890}{10^{-4}} = 907 \text{ sec}$$

As before, we can generalize to other conditions, as follows

$\dot{m}(\text{g/s})$	I(A)	F(N) (Calc.)	F(N) (measured)	$\eta$ (Calc.)	Isp(s) (Calc.)
0.1	100	0.890	(0.75)	0.256	907
0.2	100	1.196	(1.07)	0.195	607
0.3	100	1.52	(1.37)	0.194	516
0.1	60	0.652	(0.64)	0.205	664
0.1	150	1.29	(0.85)	0.385	1315

Table 3

The high current case appears anomalous (following from our overprediction of  $P_t$  in Table 1), but all others are quite reasonably predicted.